Cation Interactions and Membrane Potential Induce Conformational Changes in NaPi-IIb

Patti, Monica ; Fenollar-Ferrer, Cristina ; Werner, Andreas ; Forrest, Lucy R ; Forster, Ian C

Abstract: Voltage-dependence of Na(+)-coupled phosphate cotransporters of the SLC34 family arises from displacement of charges intrinsic to the protein and the binding/release of one Na(+) ion in response to changes in the transmembrane electric field. Candidate coordination residues for the cation at the Na1 site were previously predicted by structural modeling using the x-ray structure of dicarboxylate transporter VcINDY as template and confirmed by functional studies. Mutations at Na1 resulted in altered steady-state and presteady-state characteristics that should be mirrored in the conformational changes induced by membrane potential changes. To test this hypothesis by functional analysis, double mutants of the flounder SLC34A2 protein were constructed that contain one of the Na1-site perturbing mutations together with a substituted cysteine for fluorophore labeling, as expressed in Xenopus oocytes. The locations of the mutations were mapped onto a homology model of the flounder protein. The effects of the mutagenesis were characterized by steady-state, presteady-state, and fluorometric assays. Changes in fluorescence intensity (ΔF) in response to membrane potential steps were resolved at three previously identified positions. These fluorescence data corroborated the altered presteady-state kinetics upon perturbation of Na1, and furthermore indicated concomitant changes in the microenvironment of the respective fluorophores, as evidenced by changes in the voltage dependence and time course of ΔF. Moreover, iodide quenching experiments indicated that the aqueous nature of the fluorophore microenvironment depended on the membrane potential. These findings provide compelling evidence that membrane potential and cation interactions induce significant large-scale structural rearrangements of the protein.

DOI: https://doi.org/10.1016/j.bpj.2016.07.025

DOI: https://doi.org/10.1016/j.bpj.2016.07.025

Biophysical Journal, Volume *111*

Supplemental Information

Cation Interactions and Membrane Potential Induce Conformational Changes in NaPi-IIb

Monica Patti, Cristina Fenollar-Ferrer, Andreas Werner, Lucy R. Forrest, and Ian C. Forster

IN SUPPORTING MATERIAL

Supporting data: Structural models of flounder NaPi-IIb in outward-facing and inward-facing conformations. These models were constructed based on their homology with VcINDY. Note that the expected accuracy of the outward-facing model is likely to be higher than that of the inward-facing model.
Outward facing (also available at PMDB, with code PM0080462): NaPi-IIb Outward Facing
Inward facing: NaPi-IIb Inward Facing

Figure S1 Alignment of VcINDY and flNaPi-IIb used for structural modeling. Only regions contained in the model(s) are shown, i.e., excluding the N- and C-termini and a large extracellular loop after TM3 between the two structural repeats. The helical regions in the template VcINDY are shown as blue bars above the alignment, and the regions of predicted helicity in flNaPi-IIb are shown below the alignment; helices are labeled by transmembrane (TM) segment. Amino acids are colored by chemical property, namely acidic (red), basic (blue), polar (cyan), aromatic (gold), helix breaking (gray), while histidines are colored light green, and all other positions have a white background.

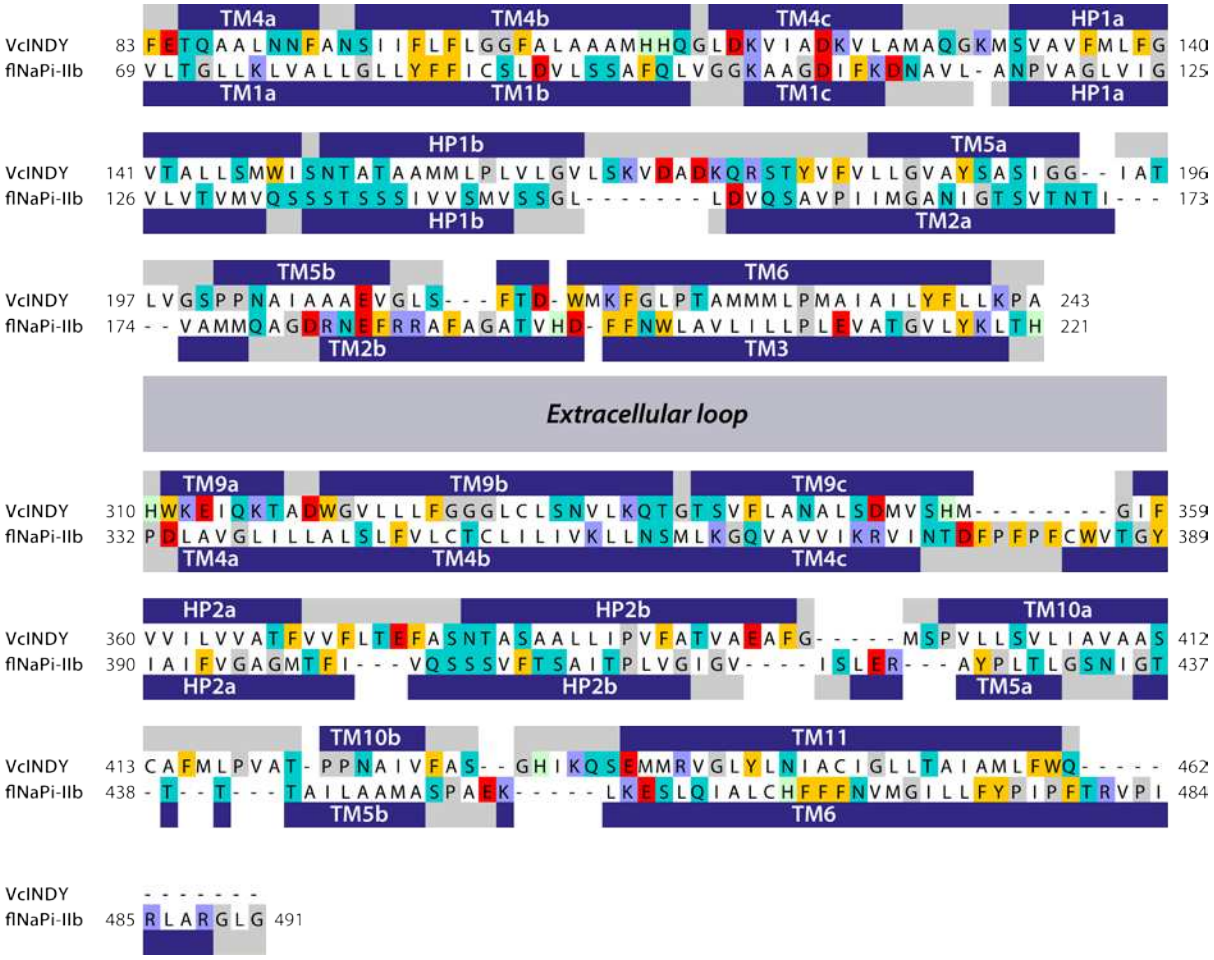

Figure S2 Steady-state electrogenic characteristics of Na1 mutants.

A) Confirmation that apparent P_i-affinity ($K_{0.5}^{Pi}$) was only marginally affected by the mutagenesis. Each data point is the pool from 4-5 representative oocytes. To determine the apparent affinity constant for P_i ($K_{0.5}^{Pi}$) the electrogenic response to different P_i concentrations added to the 100Na control solution was measured at a defined membrane potential. Oocytes were voltage-clamped to V_h = –60 mV and voltage steps were applied in the range –160 to +60 mV for typically 100 ms. To measure P_i-induced currents (I_{P_i}), the superfusate was switched from the control (100Na) solution to one containing a given concentration of P_i and when the holding current had reached a steady-state, the voltage steps were repeated. The control data set was subtracted from the data set obtained in the presence of P_i to give I_{P_i} for each [P_i] and test voltage. Estimates of $K_{0.5}^{Pi}$ were obtained by fitting data with a form of the Michaelis-Menten equation given by:

$$I_{P_i} = I_{P_i}^{max} [P_i] / ([P_i] + K_{0.5}^{Pi}) + I_{OFF} \quad \text{(S1)}$$

where $I_{P_i}^{max}$ is the maximum current attainable, I_{OFF} is a variable offset to account for uncoupled leak effects (25). To take account of the differences in expression levels between individual oocytes, data obtained from each oocyte were normalized to I_{P_i} recorded at –100 mV with 100Na and 1 mM P_i before pooling and fitting the data with Eqn. 1.

B) Comparison of activation indices for human and flounder mutants. The activation index is based on a two point assay and provides a means to determine if significant deviations from WT behavior have occurred following mutagenesis (e.g.(2)). Data for hNaPi-IIa were taken from (2) and replotted.

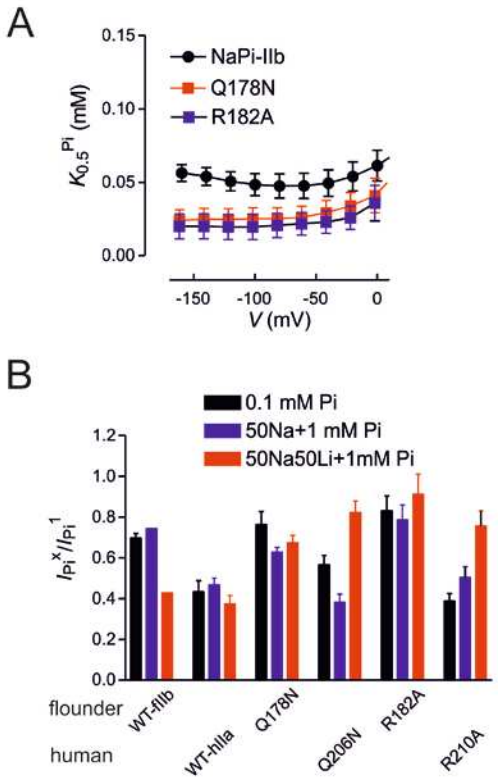

Figure S3

Current voltage (*I-V*) data for all constructs investigated in this study. The data were normalized to the response to 1 mM P_i at –100 mV for superfusion with 100Na solution. Each data point is mean±sem for n>5 oocytes. In each case, normalised data for the WT flNaPi-IIb for superfusion in 100Na in response to 1 mM Pi have been superimposed (open squares).

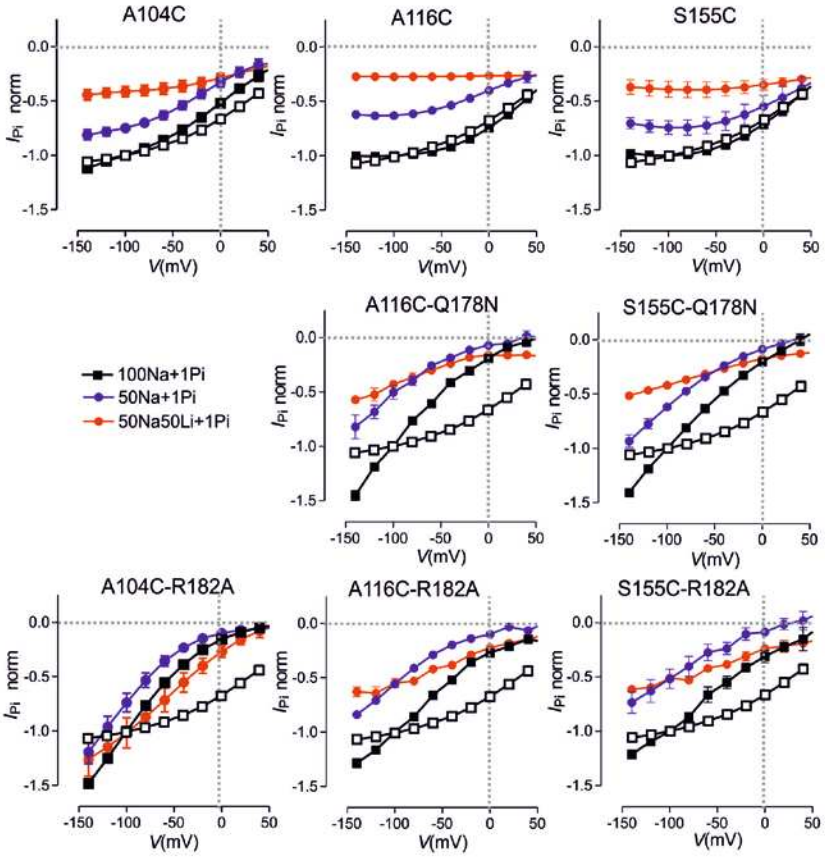

Figure S4

Voltage dependence of relaxation time constants for the WT and double mutants. Data were obtained by fitting exponentials to the presteady-state relaxation currents for two superfusion conditions. Note that the magnitude of $\tau_{ON}{}^{Q}$ is less than we obtained for the VCF recordings (Fig. 6) because these data were obtained at a higher temperature (approx. 22 ^{o}C) compared with 19-20^{o} for the former measurements. Data points pooled from n> 4 oocytes for each construct and points joined for graphical convenience only.

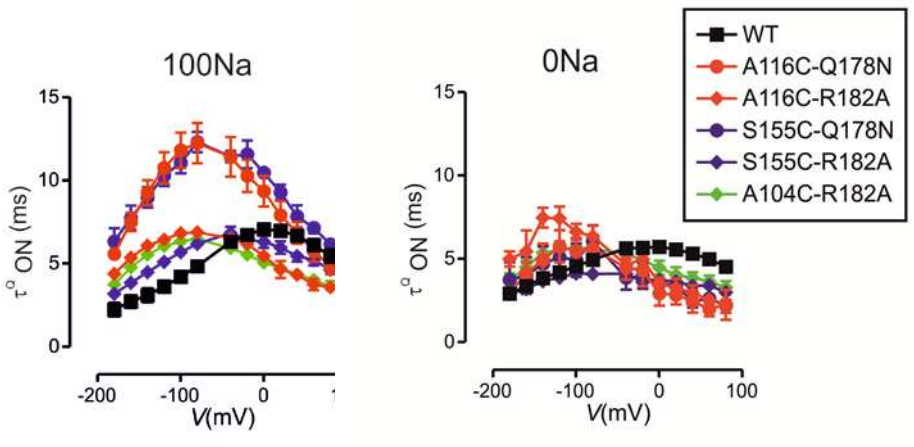

Figure S5. Quenching by I^-

A) Recordings of ΔF made from a representative oocyte expressing the labeled mutant S155C in response to voltage steps according to the standard protocol. Baseline correction was made for all traces at the –60 mV holding potential. Red traces are response at +180 mV.

B) ΔF vs V for data traces in A. These data confirm that exposure to I^- does not lead to any irreversible change in the ΔF-V characteristic.

(C) Iodide quenching displays a linear Stern-Volmer relationship. ΔF-V data were acquired from oocytes expressing A116C or S155C and labeled with MTS-TAMRA. Data were fit with a single Boltzmann function (Eqn 1) to yield the maximum change in voltage-dependent fluorescence before and after exposure to a range of [I^-]. The data are plotted as $\Delta F_{max}{}^0/\Delta F_{max}$ vs [I^-] to yield a Stern-Volmer plot, where $\Delta F_{max}{}^0$ is the mean of ΔF_{max} before and after each exposure to I^-. Each data point is the mean±sem from 4 oocytes. Linear regression fits reported slopes of 6.65 M^{-1} (A116C) and 6.08 M^{-1} (S155C) and represent the respective Stern-Volmer quenching constants (e.g. (19)).